Stimuli-Responsive Polymer Ultrathin Films with a Binary Architecture: Combined Layer-by-Layer Polyelectrolyte and Surface-Initiated Polymerization Approach

Timothy M. Fulghum,[†] Nicel C. Estillore,[†] Cong-Duan Vo,[‡] Steven P. Armes,[‡] and Rigoberto C. Advincula*,[†]

Department of Chemistry and Department of Chemical Engineering, University of Houston, Houston, Texas 77204-5003, and Department of Chemistry, University of Sheffield, Brook Hill, Sheffield S3 7HF, UK

Received July 31, 2007; Revised Manuscript Received October 30, 2007

ABSTRACT: The fabrication of a multicomponent responsive polymer ultrathin film through the combined use of the layer-by-layer (LbL) and surface-initiated polymerization (SIP) techniques is described. Through the use of the weak polyelectrolytes poly(allylamine hydrochloride) (PAH) and poly(acrylic acid) (PAA), and two alternately charged atom transfer radical polymerization (ATRP) macroinitiators, a pH-controlled membrane was prepared capable of SIP. Polymerization of *n*-isopropylacrylamide to form PNIPAM brushes on top of this membrane surface created a thermally responsive layer. The combination of these two systems created a dual control mechanism for permeability through the membrane where pH control can be utilized on the polyelectrolyte LbL layers and thermal control on the polymer brushes. A series of experiments including electrochemistry, contact angle, and in-situ ellipsometry were used to demonstrate these effects. It is possible that other stimuli-responsive systems can be designed using the two independent macromolecular assembly and synthesis protocols.

Introduction

Stimuli-responsive thin films and coatings have been of increasing interest over the past few years for both fundamental and commercial interest. Poly(*N*-isopropylacrylamide) (PNIPAM) is at the forefront of this research due to the fact that it has an interesting lower critical solution temperature (LCST) behavior that is readily observed at ∼32 °C.[1−4] In this case, the chains undergo a change in conformation, i.e., coil to globular transition as the temperature is increased above the LCST, affecting swelling and rheological properties as thin films. A number of surface-sensitive analytical techniques have been utilized for their investigation.[1−4]

Other "smart" polymer coatings have been proposed for various applications, including friction control,[5] drug delivery,[2] reversible thickness control,[6] liquid crystal command layers,[7] antireflection coatings,[8] permeability control,[1] and ion selectivity.[9] While spin-coating, self-assembled monolayers, and Langmuir−Blodgett techniques have been employed for macromolecular assembly as ultrathin films, other coating methods have gained much popularity, most notably the layer-by-layer (LbL) and surface-initiated polymerization (SIP) techniques. Surface modification through the formation of ultrathin films by the LbL technique has been demonstrated extensively since Decher and co-workers reintroduced the method in the early 1990s.[10] This technique involves the consecutive adsorption of oppositely charged species on a uniformly charged planar substrate or colloidal template for a variety of applications.[11] Repeating this simple process gives one the ability to form multilayers with precise control over total thickness, layer composition, supramolecular structure, and functionality. Films ranging from a few angstroms up to the micron level in thickness can be made reliably and reproducibly. The LbL process offers great versatility for the deposition of charged species such as polyelectrolytes,[11,12] nanoparticles,[13−15] proteins,[10,16] etc. However, other noncovalent interactions have also been utilized, such as hydrogen bonding.[13,17−19]

Stimulus responsive coatings prepared using the LbL technique have been controlled primarily by adjusting the solution or subphase pH both before and after their fabrication.[8,12,20] Strong polyelectrolytes, i.e., poly(diallyldimethylammonium chloride) (PDADMAC) and poly(sodium 4-styrenesulfonate) (PSS), usually deposit thin molecular layers when deposited from salt-free solutions due to the relatively high charge density on the polymer chains.[20] Weak polyelectrolytes, such as poly(allylamine hydrochloride) (PAH) and poly(acrylic acid) (PAA), have variable charge densities depending on the solution pH. Thus, a judicious pH selection can increase the amount of loops and tails, effectively increasing the characteristic thickness associated with each layer.[16,20−22] For strong polyelectrolytes, the same effect can be obtained through charge screening. The addition of electrolytes partially screens the charge density on the polyelectrolyte chains. By utilizing a solution pH that is close to the pK_a of a weak polyelectrolyte, thick films can be deposited that are also pH responsive.[9,20]

Work on polymer brushes has focused on both polyelectrolytes[14,15,23,24] and also thermoresponsive nonionic polymers such as PNIPAM.[1,4,25] As with the LbL modification on substrates, the interaction of substrates with their surroundings is substantially changed by the grafting of polymer brushes. Surface properties can be easily modified by varying the composition of the polymer brush, its grafting density, and its degree of polymerization. The "grafting from" or SIP approach has the benefit of placing the initiating groups directly on the surface, allowing good control over the grafting process. Various polymerization techniques have been utilized for the preparation of PNIPAM brushes. Traditional free radical polymerization has been used extensively and involves surface-bound 2,2′-azobisisobutyronitrile (AIBN) derivatives, peroxides, or photoinitiators.[1,4] Radical polymerizations create high grafting densities

[†] University of Houston.
[‡] University of Sheffield.

10.1021/ma0717136 CCC: $40.75
Published on Web 12/15/2007

Scheme 1. Substrate Modification Using the Combined LbL and SIP Methods

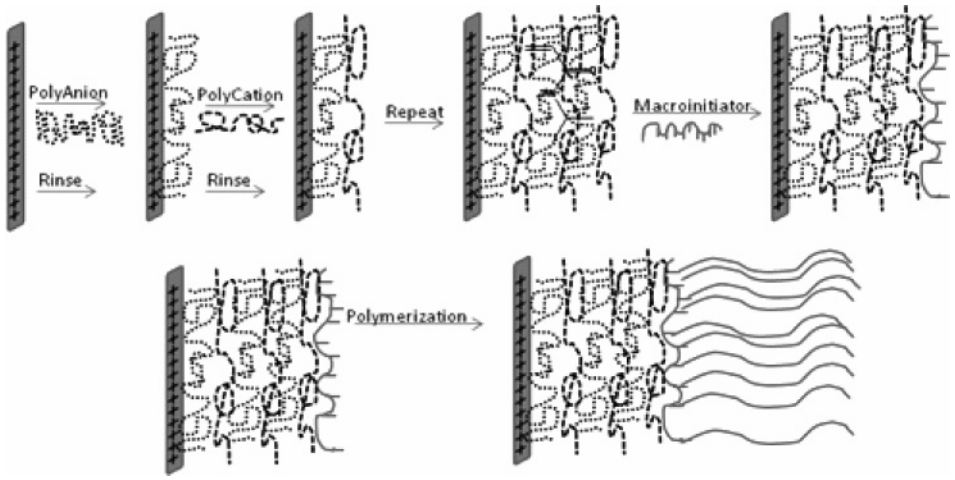

and can produce layers up to 1000 nm thick. However, this chemistry offers poor control over the brush length.[26] This disadvantage can be overcome by the use of controlled living polymerization chemistry, such as atom transfer radical polymerization (ATRP). ATRP is well suited for polymer brush synthesis due to the excellent control over brush thickness and brush polydispersity. Moreover, it allows preparation of block copolymer brushes through reinitiation of dormant chain ends and subsequently their extension with a second monomer.[24,25,27−29] The use of ATRP macroinitiators has been exploited frequently to prepare bottle brush architectures but has more recently been employed for surface functionalization and subsequent brush growth.[14,15,23,30] In this case, polyelectrolytic macroinitiators are electrostatically adsorbed onto ionic (oppositely charged) substrates from aqueous solution.

In the present study, the LbL and SIP-ATRP techniques have been combined to prepare dual sensitive surfaces. One level of control is obtained by using a poly(acrylic acid):poly(allylamine hydrochloride) (PAA:PAH) LbL system to produce a pH-sensitive ion permeable layer.[8,9] A second level of control is conferred by the use of SIP-ATRP of NIPAM to give a membrane with thermosensitive permeability (Scheme 1).[1] Various surface-sensitive spectroscopic and microscopic techniques have been utilized to characterize these new stimulus-responsive films. In principle, a well-designed LbL and SIP layer can be used to provide different levels of control or stimuli response base on functionality, composition, and architecture of the films.

Experimental Section

Materials. PAA (20 000 g/mol), PAH (65 000 g/mol), 3-aminopropyltrimethoxysilane (APS), CuBr, and *N*,*N*,*N*′,*N*″,*N*″-pentamethyldiethylenetriamine (PMDETA) were used as received from Aldrich. *N*-Isopropylacrylamide (NIPAM) was purified by recrystallization from hexanes. Methyl methacrylate (MMA) was purified by distillation. Dry solvents were freshly distilled prior to use. Milli-Q quality water (>18 MΩ resistance) was used in all procedures pertaining to the use of water. The polyelectrolyte macroinitiators (CM and AM) depicted in Figure 1 were synthesized as previously reported.[14,15,23]

Substrate Preparation Silicon, BK7 glass, and indium tin oxide (ITO) coated glass substrates were cut into 25 × 30 mm pieces and washed by hand in an Alconox (detergent) solution. The substrates were then sonicated sequentially for 15 min each with diluted Fisher ultrasonicating solution, water, acetone, and water. The substrates were then treated in piranha solution (70:30 sulfuric acid:H_2O_2) for 30 min. *(Note: extreme caution must be used when dealing with piranha solution as it reacts violently with organic materials.)* The substrates were then rinsed with copious amounts of water and dried with filtered compressed air and then subjected to argon/oxygen plasma cleaning for 3 min. The substrates were transferred to a staining jar with 0.5 vol % APS in dry toluene for a period of 1−2 h. All of the solution was discarded, and the substrates were sonicated in fresh toluene for 15 min; half of this solution was discarded, and the jar was filled with acetone and sonicated for 15 min. The substrates were then sonicated in fresh acetone for 15 min. The slides were then transferred to a staining jar with a 0.1 M HCl solution and stored until used.

Multilayer Growth. PAA (2000 g mol^{-1}) was prepared in a 1.0 g/L solution in pH adjusted water at a pH = 3.0 with HCl. PAH (70 000 g mol^{-1}) was prepared in a 1.0 g/L solution in pH adjusted water at a pH of 6 with NaOH. The macroinitiator solutions were prepared as 1.0 g/L at neutral pH. Multilayer growth was performed manually. The positively charged substrates were dipped into the PAA solution first for a period of 20 min, after which the slides were removed and rinsed with water. The substrates were then transferred to the PAH solution for a period of 20 min, after which they were rinsed and the process was repeated. The slides were not dried between layers, unless surface analysis was performed. After a set number of bilayers of PAA:PAH had been constructed, the substrates were alternately dipped in the (CM and AM) macroinitiator solutions for 20 min, with rinsing between layers.

Polymer Growth. The substrate with the PAA:PAH base layers and macroinitiator outer layers was placed into a Schlenk flask charged with 0.080 g (0.56 mmol) of CuBr and 350 μL (1.7 mmol) of PMDETA under a N_2 atmosphere. A second Schlenk flask was charged with 6.3 g (55.6 mmol) of NIPAM dissolved in 3.15 mL of water and 3.15 mL of methanol. Alternatively, the substrate was placed in a Schlenk flask charged with 0.143 g (1.0 mmol) of CuBr and 312 mg (2.0 mmol) of 2,2′-bipyridine under a N_2 atmosphere; to a second Schlenk flask was added 10 mL (93.9 mmol) of methyl methacrylate (MMA). The monomer solutions were degassed using a nitrogen purge for a period of 30−45 min and then transferred

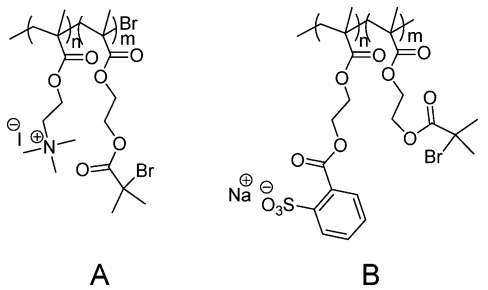

Figure 1. Chemical structures of the two polyelectrolyte ATRP macroinitiators used in this study: (A) cationic macroinitiator (CM) and (B) anionic macroinitiator (AM).

via cannula to the Schlenk flask containing the substrate and catalyst. The Schlenk flask was then transferred to a preheated oil bath at 65 °C for 12−48 h. After polymerization, the substrate was removed and placed in a Soxhlet extractor with methylene chloride or water for PMMA and PNIPAM, respectively, to remove any physically adsorbed polymer from the substrates.

Film Analysis. Fourier transform infrared (FT-IR) absorption spectra of polyelectrolyte films on silicon substrates were measured with a Digilab FTS7000 series spectrometer. Spectra (4000−700 cm^{-1}) were collected at 4 cm^{-1} resolution using a mercury−cadmium−telluride (MCT) detector with 1000 scans being averaged per spectrum. Contact angle goniometry was conducted using a KSV CAM 200 instrument (KSV Ltd.) using the bubble drop method with water.

Null ellipsometry was applied to determine the thickness of the polyelectrolyte multilayers.[31] All measurements were conducted using a null ellipsometer operating in polarizer−compensator−sample−analyzer (Multiskop, Optrel Berlin) mode. As a light source, a He−Ne laser ($\lambda = 632.8$ nm) was applied, and the angle of incidence was set to 60°. A multilayer flat film model was used to calculate polyelectrolyte multilayer thicknesses from the experimentally measured ellipsometric angles Δ and ψ, assuming a refractive index of 1.50 for the polyelectrolyte multilayers.[9] The refractive indices used for these calculations were $N = 3.873 - i0.016$ and 1.46 for the silicon substrate and native silica layer, respectively.

The film thickness was calculated using a fitting program (Elli, Optrel). In-situ ellipsometry measurements were performed on multilayer films on a silicon wafer immersed in aqueous solutions of pH = 3, 7, and 9 with a homemade glass cell. The tilt angle of the entrance and exit windows for the incident beam was set at 60° to the base window of the cell. The sample was first placed in the cell and aligned to ensure that the windows were perpendicular to the beam. The buffered solutions were then poured into the cell, and measurements were taken after 20 min. For calculation of the film thickness, a refractive index of 1.33 was used for the buffered solution.

All atomic force microscopy (AFM) images were recorded in air under ambient conditions on a PicoScan system (Agilent Technologies formerly Molecular Imaging, Corp.) equipped with an 8 × 8 μm scanner. Magnetic AC (MAC) mode (noncontact mode) was used for all imaging. A MAC lever, which is a silicon nitride-based cantilever coated with magnetic film, was used as an AFM tip.

Electrochemical cyclic voltammetry (CV) studies were performed with a Parstat 2263 (Princeton Applied Research) instrument using PowerSuite PowerCV software with a three-electrode cell at a scan rate of 100 mV/s. A platinum wire was used as the counter electrode, and Ag/AgCl (3 M KCl) was used as the reference electrode. Aqueous solutions of 0.5 M Na_2SO_4 containing 5 mM $K_3Fe(CN)_6$ buffered at pH 2.98 and 8.97 and unbuffered at pH 7.02 were prepared as electrolyte solutions. The PAH/PAA multilayer-coated ITO (working) electrodes were immersed in these solutions for 20 min prior to measurement. Likewise, the PNIPAM-coated substrates were immersed in the solution at room temperature for 20 min prior to CV. For the elevated temperature scans, the electrochemical cell was placed in a temperature-controlled water bath at 60 °C for 20 min prior to electrochemical testing.

X-ray photoelectron spectroscopy (XPS) was carried out on a Physical Electronics 5700 instrument with photoelectrons generated by the nonmonochromatic Al Kα irradiation (1486.6 eV). Photoelectrons were collected at a takeoff angle of 45° using a hemispherical analyzer operated in the fixed retard ratio mode with an energy resolution setting of 11.75 eV. The binding energy scale was calibrated prior to analysis using the Cu $2p_{3/2}$ and Ag $3d_{5/2}$ lines. Charge neutralization was ensured through cobombardment of the irradiated area with an electron beam and the use of nonmonochromated Al Kα source. This placed the adventitious C 1s peak at a binding energy of 284.6 (0.2 eV).

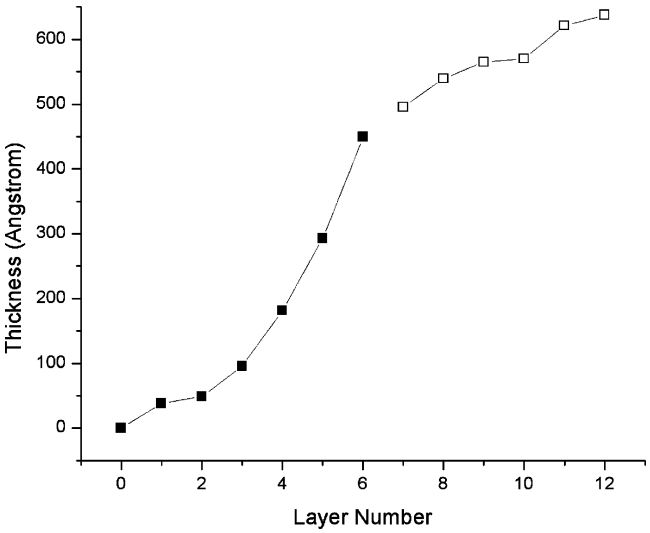

Figure 2. Ellipsometric film thickness. Alternate dipping of PAA and PAH (closed boxes) leads to an initial exponential growth of film thickness. After the third layer, the film reaches a linear growth regime. The deposition of the ATRP macroinitiators CM:AM (open boxes) is linear with a lower slope than that of the PAA:PAH layers, indicating that less material is deposited per layer.

Results and Discussion

Multilayer Growth. The LbL films were prepared by first modifying the substrates with APS for ITO, glass, and silicon substrates. The substrates were subsequently dipped into 0.1 M HCl to protonate the amine groups.[9] The substrates were then alternately dipped in the PAA and PAH solutions. After each layer was applied, the dried thickness was measured by ellipsometry (Figure 2). An average thickness of 75 Å per PAA:PAH bilayer is seen for the base deposition; this is higher than the 55 Å per bilayer reported by Shiratori et al.[22] After an initial exponential growth the film thickness grows linearly.[9,16,30] The first few layers can be attributed to the adsorption and reorganization of the polyelectrolyte at the solid substrate surface that may not be as uniformly charged and has been observed in many occasions.[11] The deposition of the alternating macroinitiator layers CMacro:AMacro is also linear but with a lower slope than the initial PAA:PAH layers. The reduced gradient indicates that the incorporated macroinitiator layers may have an inherently lower average bilayer thickness than the PAA:PAH polyelectrolytes or have a lower initiator layer surface coverage.

The FT-IR spectra shown in Figure 3 reveal a strong carbonyl stretch at 1733 cm^{-1} that is attributed to the methacrylic ester backbone of the macroinitiators.[23] The macroinitiator spectrum was recorded after five bilayers were prepared on a positively charged substrate with no base layers of PAA:PAH. The PAA:PAH bilayer spectrum shows a shoulder centered at 1720 cm^{-1} and one at 1555 cm^{-1} for the carboxylic acid (−COOH) and carboxylate ($-COO^-$), respectively.[21] Using curve-fitting software, the peak areas indicate 20% of the acrylic acid groups are present in the ionized anionic carboxylate form.[9] There is also a contribution to the shoulder at 1640 cm^{-1} from the protonated amine ($-NH_3^+$) of the PAH.[32] The PAA:PAH:CM:AM spectrum has a broadened peak between 1675 and 1750 cm^{-1}, which is due to both the carboxylic acid and ester peaks from the PAA and the macroinitiators.

Polymer Brush Growth. The prepared LbL substrates with outer layers containing ATRP macroinitiators were placed into Schlenk flasks containing CuBr and ligand under an inert atmosphere. The monomer (MMA or NIPAM) and solvent were

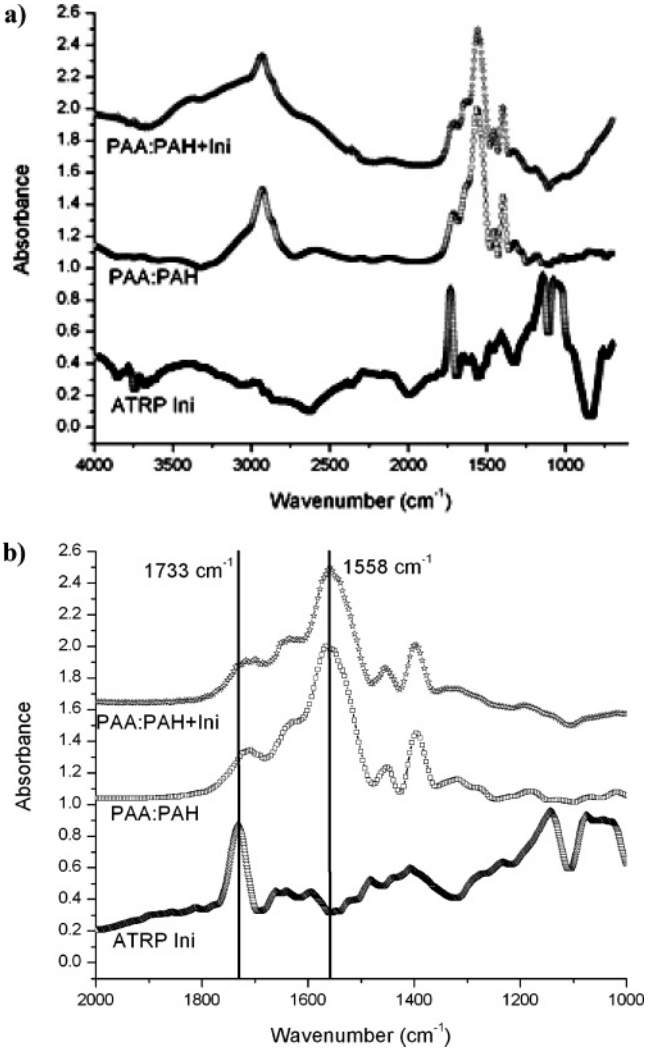

Figure 3. FT-IR analysis of initiator layers: (a) **(**lower) analysis of 3 bilayers of ATRP initiators on APS, (middle) 15 bilayers of PAA:PAH, and (upper) 20 bilayers PAA:PAH and 5 bilayers ATRP initiators (CM:AM); (b) focused spectra of the carbonyl region.

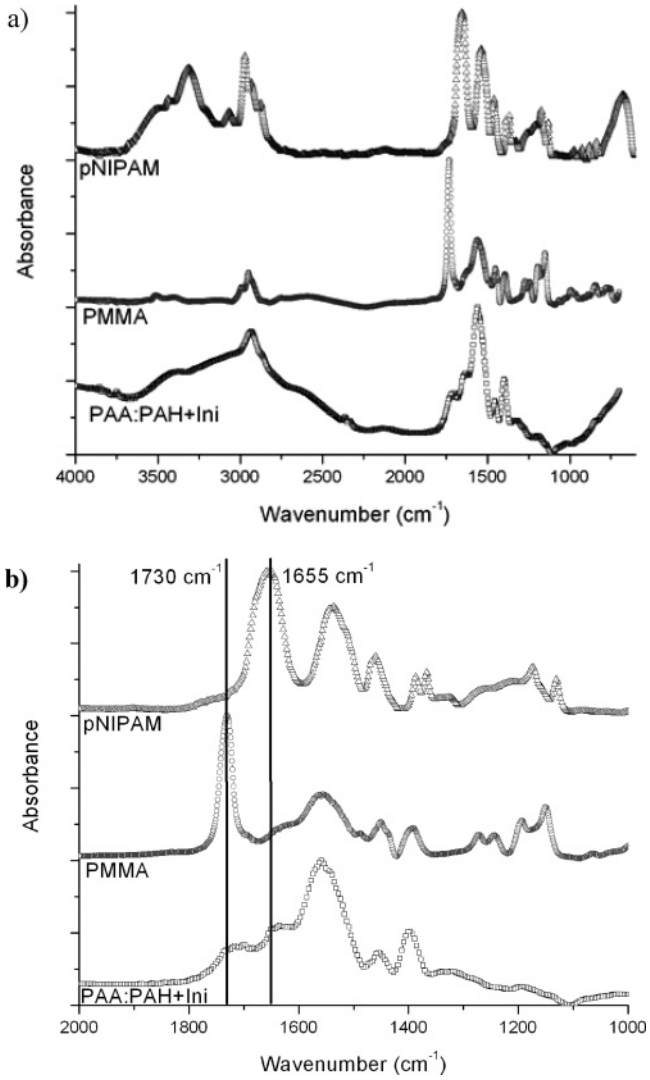

Figure 4. (a) FT-IR comparison of the macroinitiator substrate prior to polymerization (bottom), substrate after polymerization of the MMA (middle), and the substrate after polymerization of NIPAM (top). (b) Focused spectra of the carbonyl region.

placed into a second Schlenk flask and nitrogen purged for 30−45 min to degas the solution. The degassed solution was transferred via cannula to the flask containing the macroinitiator-covered substrate, and the flask was placed in a preheated oil bath. The polymerization reaction was conducted for 12−36 h, before being quenched by cooling and introducing oxygen into the reaction vessel. The substrates were then transferred to a Soxhlet extractor and purified with fresh solvent for a minimum of 12 h. The substrates were dried in a vacuum oven to remove moisture prior to recording the FT-IR spectra (Figure 4). PMMA brush was synthesized for comparison. The carbonyl region of the spectra shows the shoulder of the methacrylic acid backbone in the substrate prior to polymerization at 1720 cm^{-1}. The ratio of the carbonyl and C−H stretching vibration in the PMMA sample compared to the macroinitiator containing LbL films shows a much greater incorporation of the carbonyl-containing material due to the PMMA.[30] On the other hand, the carbonyl region for PMMA (1730 cm^{-1}) is of a higher frequency than the PNIPAM (1655 cm^{-1}), which is expected for a more stable amide.

The carboxylate peaks of the PAA:PAH multilayer are still visible at 1655 cm^{-1} in the PMMA brush film but are obscured by the amide II (C−N) stretch due to the PNIPAM brush.[2,33] The carbonyl of the methacrylic acid backbone is also complicated in the PNIPAM spectra due to amide I carbonyl backbone stretch centered at 1650 cm^{-1}.[2,33] Nevertheless, the differences between the PMMA and PNIPAM brush spectra are evident.

The surface morphology of the polymer brushes was probed with AFM imaging (Figure 5). The surface topography changed dramatically from a film with ridged features to a surface covered with globular domain features. The root-mean-square (rms) roughnesses were 7.3 and 4.3 nm for the LbL film and the PNIPAM brush, respectively. The LbL morphology is comprised of the swelled PAA:PAH multilayers and the macroinitiators with excellent wetting properties giving larger domains. After polymerization, the morphology showed globular domain features of ∼30 nm which are regularly distributed over the substrate. These globular domains reduced the overall surface roughness of the films.

XPS was performed to probe the elemental composition of the polymerized sample film to determine extent of polymerization and inclusion of CuBr salts during polymerization, i.e., not removed during Soxhlet extraction. A survey scan of the pNIPAM brush on PAA:PAH with five bilayers of CM:AM macroinitiators is seen in Figure 6. As seen in the spectra, only peaks for carbon, oxygen, nitrogen, and silicon are visible. The lack of Cu and Br peaks indicates that the catalyst was successfully removed postpolymerization. The ratio of carbon

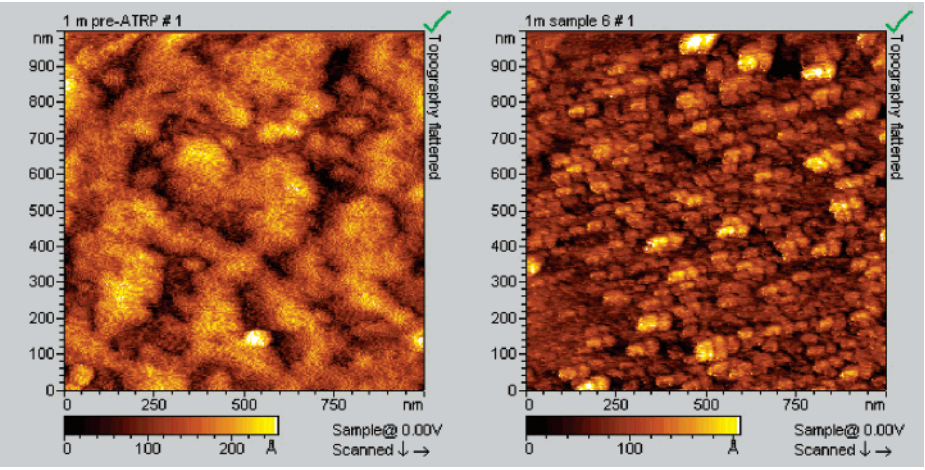

Figure 5. AFM topographic images of (left) LbL film coated with 10 bilayers of PAA:PAH and 5 bilayers of ATRP macroinitiators and (right) surface after polymerization of NIPAM.

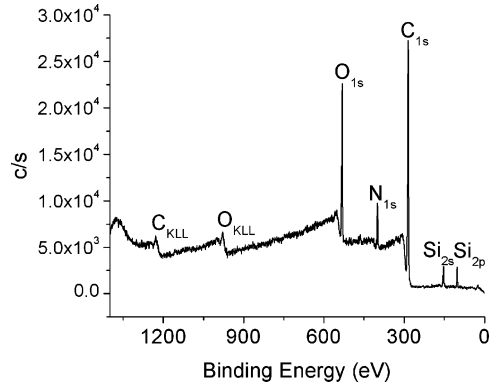

Figure 6. XPS survey scan of PNIPAM brush on 20 bilayers of PAA:PAH and 5 bilayers of macroinitiators. The lack of Cu and Br peaks is indicative of the complete removal of the ATRP catalyst.

to nitrogen in the NIPAM monomer is 6:1; however, using high-resolution spectra of the carbon and nitrogen peaks in the XPS, a ratio of 5.4:1 was determined (Supporting Information). The difference in ratio of C to N is indicative of the nonstoichiometric inclusion of PAH:PAA (4:0 and 2:1) pair composition of the LbL material. The Si peaks representative of the glass substrate is also seen.

pH Response. The PAA:PAH/macroinitiator films were prepared from aqueous solutions of 1.0 g/L PAA pH adjusted to pH = 3 with HCl, and the PAH pH was adjusted to pH = 6 with NaOH. These pH values were chosen so as to produce films that would be subsequently pH-sensitive after deposition.[8,9] pH-induced swelling was investigated using ellipsometry by immersing the PAA:PAH bilayer films in solutions at pH = 3, 7, and 9 (Figure 7). All films were partially swollen compared to the dry films. The films were most swollen at pH = 3 and least swollen at pH = 9; these results are similar to that reported by Hiller et al. and Park et al.[8,9] This swelling behavior is due to the chemical structure of the films. At pH = 3 the carboxylic acid groups in the PAA are less ionized, and the amine functionality in the PAH is more ionized than when the multilayer was prepared. Mendelsohn et al. studied the PAA:PAH LbL system over a wide pH range and showed that 80−90% of the −COOH groups are ionized during deposition with conditions similar to those described in the current study.[20] Mendelsohn et al. reported that delamination occurred below pH = 2, when the degree of ionization of the acid groups fell below 35%. Overall, these results indicated a pH responsive film to which polymer brushes can be grafted.

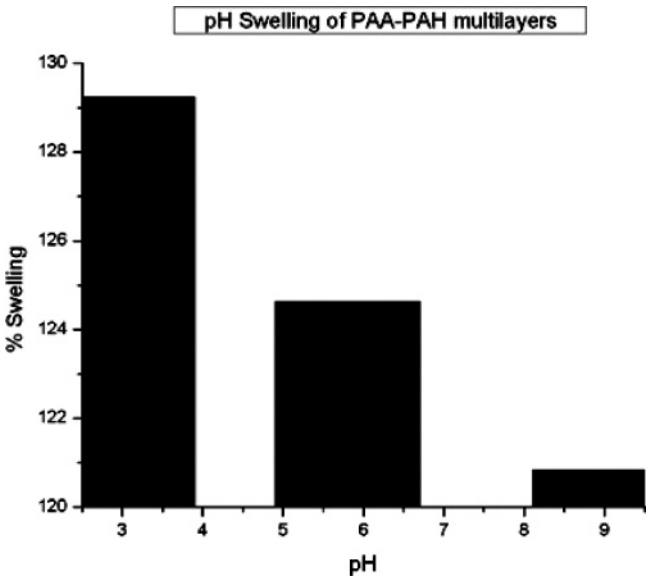

Figure 7. Variation of film thickness with solution pH. The PAA:PAH LbL film before deposition of the macroinitiators was dipped in pH 3 and swelled to ∼130% of the initial film thickness. At neutral pH, this film was still slightly swollen and at pH 9 it was least swollen, but still thicker than in the dry state.

PNIPAM Temperature Response. Investigations into the collapse of the PNIPAM brush due to its LCST transition have been performed and examined by many previous workers.[1−3] The thermoresponsive behavior of PNIPAM brushes differs from that of isolated chains in dilute aqueous solution. Because of the density and arrangement of the polymer chains in the brush conformations, the chain collapse is observed at a higher temperature than in dilute solution.[3] To probe this, the PNIPAM brush coated substrates were dried in a vacuum oven for 6 h prior to analysis by contact angle goniometry. Water contact angle measurements were made by placing the substrate at room temperature on the sample stage and recording the contact angle for low-temperature measurements. The contact angle was again recorded after the substrate had been immersed in water at 40 °C for 20 min, after which it was blown dry and measured immediately.

A mean water contact angle of 17.8° was obtained for the samples after rinsing with Milli-Q water at 20 °C, followed by air drying. In contrast, a mean contact angle of 62.6° was obtained after immersion in water at 40 °C for 20 min, followed by air drying. A representative sample after the room temper-

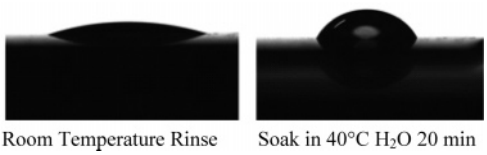

Figure 8. Water contact angle. The left-hand image is that of the PNIPAM brush after rinsing with water at 20 °C and then drying with filtered air. The right-hand image is that of the PNIPAM brush after soaking in water for 20 min at 40 °C, followed by air drying.

ature rinse and the hot water soak is shown in Figure 8. Balamarugan et al.[3] and Plunkett et al.[34] have each studied the collapse of PNIPAM brushes using surface plasmon resonance and quartz crystal microbalance, respectively. These studies indicate that the brush collapse is a more gradual transition than that observed in dilute aqueous solution.[3,34] This accounts for the more hydrophobic contact angle observed at a temperature less than that required for complete collapse of the brush.[3] In order to cause complete collapse of the brush, a temperature of 40 °C was employed. This is substantially higher than the LCST of 32 °C typically observed in dilute aqueous solution and comparable to the higher transition reported by both Plunkett and Balamurugan.[3,34] Film thicknesses of dry samples were measured by ellipsometry after water contact angle measurements were completed. The brush thicknesses were reduced by ~80 Å after immersion at 40 °C, which corresponds to a 15% reduction in thickness.[3,34]

Selective Permeability at Different pH and Temperatures. Films were examined both before polymerization and after surface polymerization to determine their response to external stimuli and how this affected their permeability. Carboxylate ($-COO^-$), carboxylic acid ($-COOH$), amine ($-NH_2$), and protonated amine ($-NH_3^+$) features were observed in the FT-IR spectra of the LbL films. By varying the pH of the dipping solution, the total film charge can be adjusted to give a net positive or net negative surface charge.[9] This pH regulated permeability of the underlying LbL multilayer can be coupled with the thermal response and permeability of the PNIPAM brush.[1,2] Ionic permeability was determined using $Fe(CN_6)^{3-}$ anions as a probe. The results of these studies are shown in Figure 9. LbL films comprising just the PAA:PAH multilayers were examined first to compare with previous results by Park et al.[9] The CV showed a well-behaved redox couple as expected for $K_3Fe(CN)_6$ in LbL films (Figure 9a). The permeability confirmed that the anionic probe diffused freely through the film at pH = 3 but had less mobility at neutral pH, as indicated by a decrease of 20% in the maximum current density. There was almost zero mobility of the anionic probe at pH = 9, with less than 10% of the current density being observed at this pH compared to that at pH = 3. This reduced current density at higher pH observed for the anionic probe corresponds with previous permeability data reported for PAA:PAH bilayers.[9] Consistently, the oxidation and reduction peaks were reversible for all cases and did not shift very much with pH, indicating a typical diffusion-limited ion transport (electrolyte) behavior. For the PNIPAM brush modified films, they also exhibited a pH-regulated permeability, but in this case, the current density was different with a lowering of the oxidation and reduction peaks especially at pH = 6 and 9. This shift, especially with the reduction wave, is attributed to the contribution of the amide group toward the Fe(II/III) complex transport to the membrane since the amide group is well-known to act as a ligand.[32] The

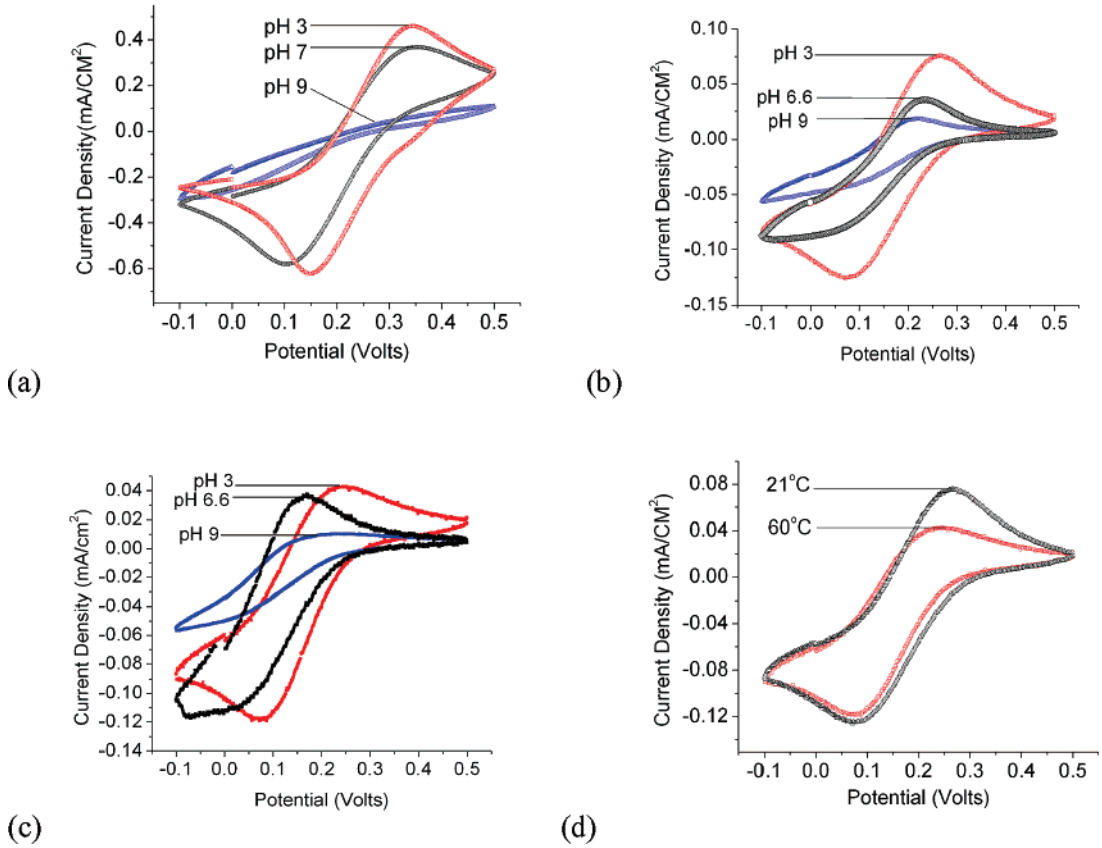

Figure 9. Cyclic voltammetry: (a) pH-dependent scans on $Fe(CN_6)^{3-}$ permeability of PAA:PAH LbL architecture at room temperature; (b) pH-dependent scans on $Fe(CN_6)^{3-}$ permeability of PAA:PAH:PNIPAM LbL:Brush architecture at room temperature; (c) pH-dependent scans on $Fe(CN_6)^{3-}$ permeability of PAA:PAH:CA:CM:PNIPAM LbL:Brush architecture at 60 °C; (d) comparative scan of PAA:PAH:CA:CM:PNIPAM at pH = 3 at room temperature and 60 °C.

CV curves were not as well-behaved reversibly, indicating a more surface-limited diffusion behavior of the ions in the presence of the PNIPAM brush. Still the highest mobility was observed at the lowest pH when the film is most swelled. To test the effect of temperature, similar experiments were performed for the films with pH = 3 and at 20 and 60 °C. After scanning at room temperature the electrochemical cell was immersed in a preheated water bath at a temperature of 60 °C, in order to maximize the collapse of the PNIPAM brush and hence reduce its porosity. Comparison of the room temperature and elevated temperature experiments indicated a reduction in the maximum current density by 45% at the elevated temperature 60 °C. This is a consequence of the collapse of the PNIPAM brush which limits the ion transport through the membrane because of increased hydrophobicity, although maintaining the electron-transport properties through the electrolytes. Thus, the maximum current density always decreases from acidic pH to neutral pH and is larger for the PNIPAM brush substrate than the pure PAA:PAH LbL-coated substrate. Temperature changes the permeability of the membrane primarily by limiting ion transport. In principle, smart membranes can be designed to have both pH- and temperature-dependent properties with respect to ion and electron transport properties for practical applications.

Conclusions

Multiple stimuli selectively permeable substrates have been created through the combination of the LbL multilayer growth of PAA:PAH coatings combined with the SIP-ATRP method utilizing polyelectrolyte macroinitiators. It was demonstrated that a pH switchable LbL membrane can be fabricated with permeability control by altering the net charge of the membrane. This was combined with a thermally adjustable coating polymerized on top of the LbL layers whose permeability was controlled through a thermally sensitive transition. More work with the current architecture is planned with investigations into controlled release of dyes and particles. Also, further investigations into the use of different thermally responsive polymer brush architectures and other alternate polyelectrolyte pairs should offer insight into the structure−property relationships for dual control of these stimuli-responsive polymer films.

Acknowledgment. Support for this work from NSF CHE-03-04807, DMR-03-15565, ACS-PRF-45853-AC7 Grant, and the Alliance for Nanohealth of Texas is gratefully acknowledged. The authors also thank Agilent Technologies Inc., Optrel GmBH, and Varian Inc. for help with technical assistance on the AFM, ellipsometer, and FT-IR measurements. S.P.A. is the recipient of a five-year Royal Society-Wolfson Research Merit Award. S.P.A. thanks EPSRC for post-doctoral support of CDV (GR/S60419).

Supporting Information Available: Atomic force microscopy images of brush films, high-resolution XPS scans, and more cyclic voltammetry of the films. This material is available free of charge via the Internet at http://pubs.acs.org.

References and Notes

(1) Rao, G. V. R.; Krug, M. E.; Balamurugan, S.; Xu, H. F.; Xu, Q.; Lopez, G. P. *Chem. Mater.* **2002**, *14*, 5075−5080.
(2) Kim, J. H.; Lee, T. R. *Drug Dev. Res.* **2006**, *67*, 61−69.
(3) Balamurugan, S.; Mendez, S.; Balamurugan, S. S.; O'Brien, M. J.; Lopez, G. P. *Langmuir* **2003**, *19*, 2545−2549.
(4) Ista, L. K.; Mendez, S.; Perez-Luna, V. H.; Lopez, G. P. *Langmuir* **2001**, *17*, 2552−2555.
(5) Chang, D. P.; Dolbow, J. E.; Zauscher, S. *Langmuir* **2007**, *23*, 250−257.
(6) Harnish, B.; Robinson, J. T.; Pei, Z. C.; Ramstrom, O.; Yan, M. D. *Chem. Mater.* **2005**, *17*, 4092−4096.
(7) Park, M. K.; Advincula, R. C. *Langmuir* **2002**, *18*, 4532−4535.
(8) Hiller, J.; Rubner, M. F. *Macromolecules* **2003**, *36*, 4078−4083.
(9) Park, M. K.; Deng, S.; Advincula, R. C. *J. Am. Chem. Soc.* **2004**, *126*, 13723−13731.
(10) Lvov, Y.; Decher, G.; Sukhorukov, G. *Macromolecules* **1993**, *26*, 5396−5399.
(11) Advincula, R.; Park, M. K.; Baba, A.; Kaneko, F. *Langmuir* **2003**, *19*, 654−665.
(12) Park, M. K.; Deng, S. X.; Advincula, R. C. *Langmuir* **2005**, *21*, 5272−5277.
(13) Hao, E. C.; Lian, T. Q. *Langmuir* **2000**, *16*, 7879−7881.
(14) Chen, X. Y.; Armes, S. P.; Greaves, S. J.; Watts, J. F. *Langmuir* **2004**, *20*, 587−595.
(15) Chen, X. Y.; Armes, S. P. *Adv. Mater.* **2003**, *15*, 1558-+.
(16) Fery, A.; Scholer, B.; Cassagneau, T.; Caruso, F. *Langmuir* **2001**, *17*, 3779−3783.
(17) Patton, D.; Locklin, J.; Meredith, M.; Xin, Y.; Advincula, R. *Chem. Mater.* **2004**, *16*, 5063−5070.
(18) Stockton, W. B.; Rubner, M. F. *Macromolecules* **1997**, *30*, 2717−2725.
(19) Wang, L. Y.; Wang, Z. Q.; Zhang, X.; Shen, J. C.; Chi, L. F.; Fuchs, H. *Macromol. Rapid Commun.* **1997**, *18*, 509−514.
(20) Mendelsohn, J. D.; Barrett, C. J.; Chan, V. V.; Pal, A. J.; Mayes, A. M.; Rubner, M. F. *Langmuir* **2000**, *16*, 5017−5023.
(21) Choi, J.; Rubner, M. F. *Macromolecules* **2005**, *38*, 116−124.
(22) Shiratori, S. S.; Rubner, M. F. *Macromolecules* **2000**, *33*, 4213−4219.
(23) Vo, C. D.; Schmid, A.; Armes, S. P.; Sakai, K.; Biggs, S. *Langmuir* **2007**, *23*, 408−413.
(24) Ayres, N.; Cyrus, C. D.; Brittain, W. J. *Langmuir* **2007**, *23*, 3744−3749.
(25) Yim, H.; Kent, M. S.; Mendez, S.; Lopez, G. P.; Satija, S.; Seo, Y. *Macromolecules* **2006**, *39*, 3420−3426.
(26) Uhlmann, P.; Ionov, L.; Houbenov, N.; Nitschke, M.; Grundke, K.; Motornov, M.; Minko, S.; Stamm, M. *Prog. Org. Coat.* **2006**, *55*, 168−174.
(27) Gao, H. F.; Matyjaszewski, K. *Macromolecules* **2007**, *40*, 399−401.
(28) Gao, H. F.; Ohno, S.; Matyjaszewski, K. *J. Am. Chem. Soc.* **2006**, *128*, 15111−15113.
(29) Xia, J. H.; Matyjaszewski, K. *Macromolecules* **1999**, *32*, 2434−2437.
(30) Fulghum, T. M.; Patton, D. L.; Advincula, R. C. *Langmuir* **2006**, *22*, 8397−8402.
(31) Motschmann, H.; Stamm, M.; Toprakcioglu, C. *Macromolecules* **1991**, *24*, 3681−3688.
(32) Amaral, I. F.; Granja, P. L.; Barbosa, M. A. *J. Biomater. Sci., Polym. Ed.* **2005**, *16*, 1575−1593.
(33) Buffeteau, T.; Le Calvez, E.; Castano, S.; Desbat, B.; Blaudez, D.; Dufourcq, J. *J. Phys. Chem. B* **2000**, *104*, 4537−4544.
(34) Plunkett, K. N.; Zhu, X.; Moore, J. S.; Leckband, D. E. *Langmuir* **2006**, *22*, 4259−4266.

MA0717136